Magnetic imaging

2001 J. Phys.: Condens. Matter 13 11163

(http://iopscience.iop.org/0953-8984/13/49/305)

INSTITUTE OF PHYSICS PUBLISHING JOURNAL OF PHYSICS: CONDENSED MATTER

J. Phys.: Condens. Matter **13** (2001) 11163–11180 PII: S0953-8984(01)29434-X

Magnetic imaging

F U Hillebrecht

Max-Planck-Institut für Mikrostrukturphysik, Weinberg 2, 06120 Halle, Germany

Received 3 October 2001 , in final form 8 November 2001
Published 10 December 2001
Online at stacks.iop.org/JPhysCM/13/11163

Abstract

The present status of techniques for imaging magnetic micro- and nanostructures by microscopy utilizing synchrotron radiation is reviewed. In general, these techniques are based on magnetic dichroism in soft x-ray spectroscopy, i.e. a dependence of the optical properties on the relative orientation of light polarization and the magnetic order parameter. They allow for a higher spatial resolution than microscopic techniques using visible optics. Furthermore, excitation by soft x-rays tuned to core level edges provides elemental specificity, i.e. the possibility to probe differentially the magnetic properties of different chemical species present in the sample.

1. Introduction

The long-range magnetic order of solids has two aspects, microscopic and macroscopic. First of all, magnetism is a specific property of the electronic structure. Therefore, a satisfactory description of magnetism can only be achieved from a microscopic understanding of the electronic structure. Such information is obtained from studies of magnetic materials in a well defined magnetic state. This implies that the sample under study has to be in a magnetic state which is uniform and known over the volume of the sample probed by the experiment. Such a homogenous state is normally not the ground state of a magnetic material: Without special treatment, a piece of a ferromagnetic material will consist of many domains with different magnetization directions so as to minimize the total energy [1]. To minimze the magnetostatic energy, which is a significant contribution ot the total energy, closure domains are formed which avoid magnetic field reaching out into the surroundings of the sample. The properties of any magnetic material, in particular the shape of the hysteresis loop, depend sensitively on the presence and size of magnetic domains. However, even though the domain structure is influenced by macroscopic properties, e.g. the sample size and shape, it also reflects microscopic properties such as the magnetic anisotropy. Therefore, the domain structure is an important aspect which has to be known for a comprehensive understanding of such materials. To define magnetic domains formally, one can say that domains are regions within a magnetic material which show translational symmetry *including* the magnetic order. Any material with long-range magnetic order, ferro- or antiferromagnetic, may show domains.

Any experimental technique which probes the magnetization state may be used to image the domain pattern. A standard approach for imaging magnetic domains is magneto-optics, where the dependence of the optical properties on the magnetization state is used in an optical microscope. Contrast between regions with different magnetization arises from a finite off-diagonal element of the dielectric tensor, which depends on the sample magnetization. The microscopic reason for this effect is the combined influence of spin–orbit interaction and the spin polarization of the valence band. In the optical regime, electronic transitions are only possible between the occupied and the unoccupied part of the valence band. Since the spin–orbit interaction is generally small for the d states of transition metals, the magnitude of the effects available for domain imaging are small. By using soft x-ray energies instead of photons in the visible regime, one has much larger effects available, since the photon energy is sufficient to excite electrons from core levels, which have a large spin–orbit interaction, to the unoccupied part of the valence band. Another reason for using soft x-rays is connected to the resolution which may be obtained: as the wavelength of the photons or electrons—in the case where electrons are used for imaging—is much smaller than that of visible light, the ultimate resolution is higher than in the visible regime. Finally, since magnetic contrast is only observed for excitation at core level edges, it is easily possible to obtain information differentially for different chemical species present in the sample. These attractive features are the motivation for the rapid development which is taking place in this field. In this paper the present status of imaging magnetic domains by techniques based on magnetic dichroism in x-ray spectroscopy is reviewed.

Core level excitations may be studied in many different ways. The most simple experimental approach is absorption spectroscopy, which requires a tuneable radiation source providing photon energies sufficient to excite electrons from inner shells to unoccupied levels. Synchrotron radiation offers exactly these properties, and therefore absorption spectroscopy has flourished enormously due to the availability of these versatile radiation sources. In addition to the tunability, synchrotron radiation is intrinsically polarized. It is this combination of tuneability and polarization of synchrotron radiation which provided the basis for the development of magnetic dichroism spectroscopy for magnetic materials.

In the context of core level spectroscopy, the term magnetic dichroism describes any kind of a dependence of a core level spectrum on the relative orientation of light polarization and magnetic order. Such dependencies have been explored since the late 1980s, both theoretically and experimentally. Figure 1 shows magnetic dichroism as measured at the Ni 2p absorption threshold [2]. The spectrum shows sharp structures arsing from excitation of a 2p core electron to the narrow band of unoccupied states, which are called 'white lines', and a step-like increase of the absorption for photon energies well above the edges. Magnetic dichroism is evident in the change of the absorption spectra seen in figure 1, which are associated with a change of the either the sample magnetization or the helicity of the light. The change of the absorption coefficient at the Ni $2p_{3/2}$ edge is about 6%, and may be as large as 50% for Fe [3]. As mentioned above, the origin of this dichroism lies in the combined influence of spin–orbit interaction and the spin polarization of the unoccupied states above the Fermi level. Excitation by circularly polarized light imposes a selection rule for the magnetic quantum number m. For excitation from a level with non-zero orbital momentum quantum number, this leads to a spin-dependent excitation cross section. In a ferromagnet the unoccupied states are spin-polarized just as the occupied ones are, so that the absorption cross section changes when either the sample magnetization or the light helicity is reversed. A detailed understanding of this effect is the subject of a different paper in this issue, and will not be discussed here. In this review, we describe how this effect is used to determine the magnetic domain structure of a multi-domain sample.

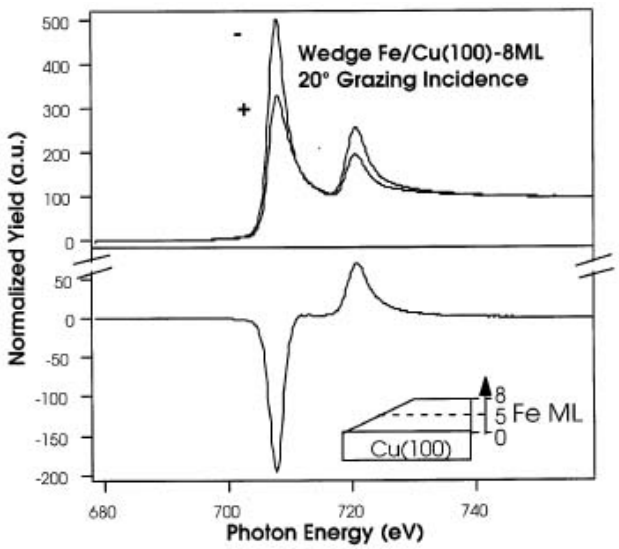

Figure 1. Magnetic circular dichroism in the Ni 2p absorption spectrum (from [2]).

It is clear that a spatially resolved measurement of the absorption coefficient yields information on the local magnetization. There are two ways to implement an imaging of the domain structure. One way is to construct an imaging system for soft x-ray wavelengths, i.e. an x-ray microscope, which allows us to directly measure the absorption or reflection coefficient in a spatially resolved way. Another approach is based on the fact that the absorption process can be monitored by emission of secondary electrons: inner shell vacancies which are created by absorption of x-ray photons decay primarily via Auger processes. So, even though the electron excited in the primary transition cannot be emitted into vacuum since its energy is just above the Fermi level, the subsequent decay of the inner shell vacancy leads to hot electrons whose energies are far above the vacuum level. Furthermore, the energetic electrons arising from the Auger decay undergo inelastic collisions on their way to the surface, generating a large number of lower-energy electrons which still have suffient energy to overcome the sample work function. The total number of electrons emitted from the sample is a (relative) measure for the absorption coefficient [4]. Imaging of magnetic domains by magnetic dichroism requires only information on the local variations of the absorption coeffcient, and this can be easily obtained from the locally emitted sample current. For this purpose the sample is illuminated at a standard synchrotron beam line, and the imaging is performed by a photoemission electron microscope, abbreviated to PEEM. Both methods—x-ray microscopy and photoemission microscopy—are based on the use of synchrotron radiation. An attractive feature of x-ray microscopy is the possibility to apply a magnetic field to the sample, which is difficult in a photoemission microscope. On the other hand, photoemission microscopy has the advantage that the sample preparation is comparatively simple since it is not necessary to use a sample which is transparent for the radiation. In terms of the achievable resolution the last word is not spoken yet as both types of instrument are still undergoing development. In some issues of micromagnetism, already the currently available resolution appears to be sufficient. In practice, the choice of the method depends on the type of information which one wants to obtain from the experiment, and sometimes—not unimportant in a field which is close to technical applications—on which facility is available at the shortest notice.

2. X-ray microscopy in transmission and reflection

X-ray transmission microscopes have been developed over the last few years mainly for the study of biological materials in the so-called water window, i.e. in the energy regime between the C and O 1s edges (280–530 eV). By modifying the beamline optics such that it accepts light emitted above or below the plane of the electron orbit in the storage ring, one can operate the microscope with circularly polarized light. This approach has been realized at the soft x-ray microscope installed at BESSY I [5]. This instrument uses zone plate optics for imaging, which inherently comprises a wavelength selection. The sample is normal to the optical axis of the microscope, and the microscope image shows lateral variations of the sample transmission for the wavelength to which the microscope is tuned. As the light is transmitted near to the normal of the sample, circularly polarized light leads to magnetic contrast for domains with magnetization perpendicular to the sample plane. Figure 2 shows a domain image obtained for a Fe–Gd multilayer, consisting of 75 periods of 0.43 nm Fe/0.48 nm Gd deposited by sputtering on a 30 nm Si_3N_4 membrane. The photon energy was tuned to the Fe $2p_{3/2}$ absorption edge. The dark and bright stripes show domains in which the magnetization points into or out of the film. The resolution in this image appears to be below 100 nm. The domains have a width of about 220 nm, and at points where three stripes are joined they form angles close to 120°. This is caused by dipolar repulsion between equally magnetized domains.

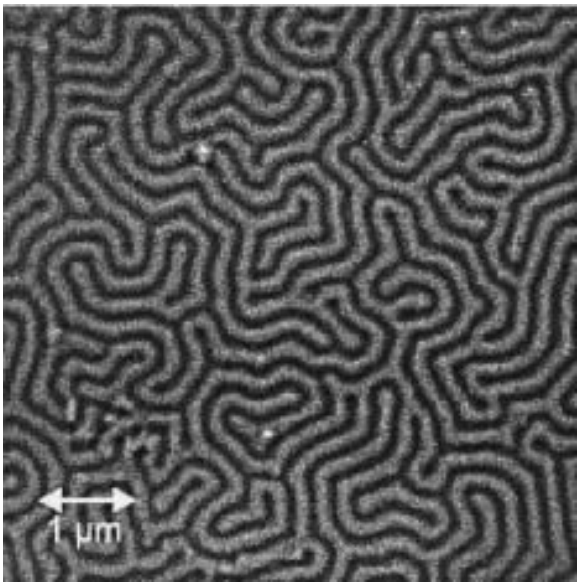

Figure 2. Image of perpendicular domains in a Fe/Gd multilayer supported on a Si_3N_4 membrane from an x-ray transmission microscope. The image was taken with circularly polarized light tuned to the Fe $2p_{3/2}$ edge, and a field of 80 Oe was applied perpendicular to the sample (from [5]).

The high resolution and fast data acquisition offered by this technique are attractive characteristics. Furthermore, the possibility to apply a magnetic field is highly desirable for studies on magnetic materials. The tradeoff is the necessity to work with samples thin enough so that there is a significant transmission at the soft x-ray energies used for imaging. This implies that in general one needs specially prepared samples. This limitation can be avoided by working in reflection, since the light reflected specularly from the surface of a magnetic material exhibits dichroic effects analogous to those in absorption. Since the reflectivity for

x-rays is in general small, such a microscope has to work with grazing incidence, which complicates the optical setup. The first experiment on domain imaging in the reflection mode has been carried out at the soft x-ray scanning microscope operating at Hasylab in Hamburg [6, 7]. This instrument focuses the x-ray beam to a diameter of less than 1 μm by employing a ellipsoidal ring mirror. An image is constructed by scanning the sample under the beam, and measuring the reflectivity at each sample position. Figure 3 shows a domain image obtained on an Fe sample with photons tuned to the Fe 3p threshold. Here, the transverse magneto-optic Kerr effect was used: for linear p-polarized radiation at oblique incidence, the reflected intensity changes for the sample magnetization switching between the directions normal on the plane of incidence [8, 9]. The resolution achieved in this image is about 1 μm. Reflection microscopy does not require thin transmitting samples; however, the surface has to have a good reflectivity ('optical quality'). To maintain a sufficient reflectivity, the angle of incidence was set to 60°. Therefore, to stay in focus while scanning, the sample is not only scanned perpendicular to the optical axis but also parallel to it so that the illuminated spot is always at the same distance from the ellipsoidal mirror. In this microscope it is also possible to apply a magnetic field, and spatially resolved hysteresis curves have been recorded. Since the magnetic dichroism in the reflected light depends in a more complicated fashion on both the real and imaginary part of the off-diagonal element of the dielectric tensor, as well as on the diagonal element, quantitative information on the magnitude of magnetic moments is not easily accessible.

3. Magnetic imaging by photoemission microscopy (PEEM)

In a photoemission electron microscope, an image of the sample surface is formed by electrons released from the sample as a result of irradiation by UV or soft x-ray photons [10–14]. The main components of a photoemission microscope are shown schematically in figure 4. The sample and the first electrode form a plane capacitor, and an accelerating voltage is applied between its plates. This field strength is commonly of the order of 25–40 kV cm^{-1}. Due to this accelerating field, the trajectories of the electrons emitted from the sample appear as coming from a point lying below the sample surface. This constitutes the first magnifying stage of the microscope. It is followed by additional magnifying and transfer stages which generate an enlarged image of the local electron yield on an image detector. This detector may be a channelplate with fluorescent screen, viewed by a CCD camera, or a CCD chip placed directly in the electron beam. In the first generation of instruments, there is no explicit energy analysis of the electrons, although the energy-dependent transmission emphasizes low-energy electrons. Contrast arises from a local variations of the electron yield, which may be caused by a number of different mechanisms. For photon energies close to the photothreshold, local variations of the work function lead to large differences of the electron yield. This aspect was used in studies of adsorption and reaction kinetics on surfaces [11]. Topographic details, i.e. cracks, particles on the surface, or steps are observable because they modifiy the electric field close to the sample surface. For soft x-ray energies, the electron yield is largely determined by the absorption coefficient, as discussed above. This can be used to image surfaces of chemically inhomogeneous materials by tuning the photon energy to different absorption edges. For a magnetic system the absorption edges depend on the relative orientation of the magnetic order parameter, e.g. the magnetization of a ferromagnet, and light polarization. Therefore, by measuring the local absorption coefficient via the electron yield in a photoemission microscope, one obtains a map of the magnetization close to the sample surface. This can only be done using synchrotron radiation since the light has to be tuned to the absorption edge, and it has to be polarized. For ferromagnetic materials, usually circularly polarized light is used, although

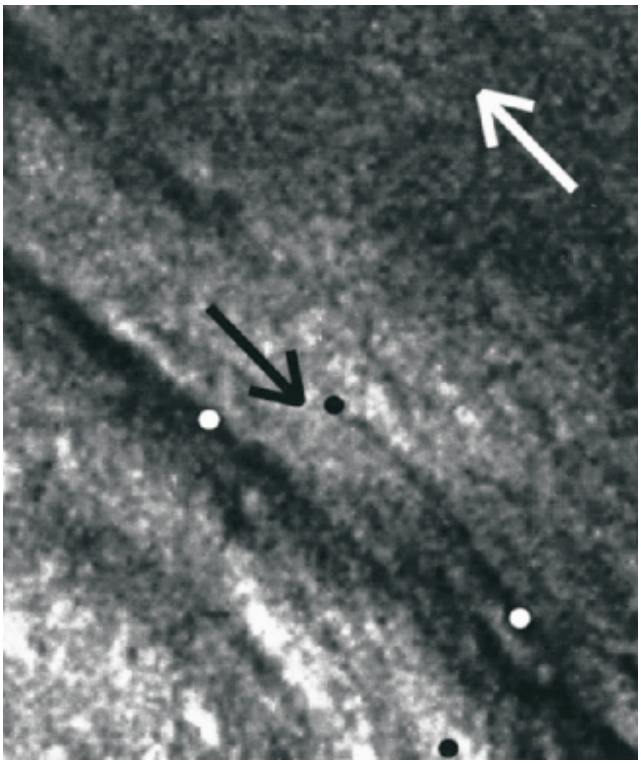

Figure 3. Scanning x-ray reflection microscopy of a 200 nm Fe film obtained by subtracting an image taken at 56.5 eV from the data at 53.7 eV and normalizing to the sum. The field of view is about 200 μm wide. At the positions marked by dots, energy dependent reflectivity measurements were performed, showing the transverse magnetic Kerr effect at the Fe 3p edge, in agreement with data from a magnetically saturated sample. The arrows indicate the magnetization in the different domains [7].

in certain cases domain images can also be obtained by excitation with linearly polarized light. Lately, linearly polarized light has been used to investigate antiferromagnetic domains of transition metal oxides, which are collinear antiferromagnets.

Contrast arising from the presence of different magnetic domains is always superimposed on contrast coming from other sources, e.g. work function variations or topographic features. Therefore, to identify any observed contrast with a magnetic cause, a way to remove contrast coming from other sources is required. When imaging ferromagnetic surfaces under excitation by circularly polarized light, this can be done by reversing the helicity of the light. Undulator sources which allow a change of the light polarization by adjusting the phase between the horizontal and vertical periodic magnetic fields are the optimum solution for this purpose.

An important aspect when comparing different experimental techniques for determining the topography of magnetic domains is the time required for data acquisition. Table 1 compares a number of synchrotron-based techniques with a selection of a few techniques which do not require synchrotron radiation. If the light source used for excitation offers sufficient intensity, PEEM images may be acquired within less than a minute. In favourable cases it is possible to record images dynamically with video rate while changing experimental parameters, such as temperature, or even—within a limited range—while a magnetic field is being applied [15]. Scanning microscopes are in principle slower since the image is built up sequentially pixel by

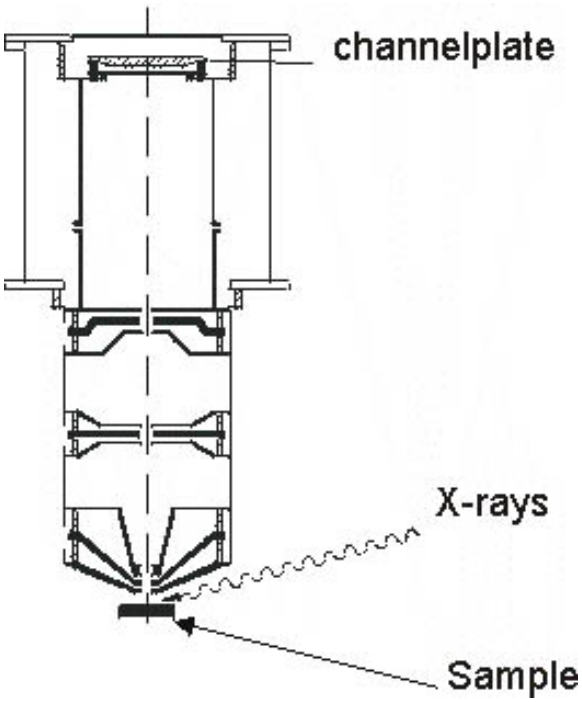

Figure 4. Schematic layout of a photoemission microscope.

pixel. Scanning electron microscopy with polarization analysis (SEMPA) requires about 10 minutes for an image [16]. The x-ray scanning microscopes (XSM) available to date probably are close to achieving a similar speed.

Table 1. Imaging techniques for magnetic domains.

	Excitation	Resolution (nm)	Chem. Spec.	AF-spec.	Probing depth (ML)	Remarks
PEEM	UV	30 (Opt.: 7 nm)	–	yes	–	'real' samples
PEEM	Synchr.	100	yes	yes	0.1	'real' samples
XSM	Synchr.	500	yes	yes	0.5	Magn. field
XTM	Synchr.	20	yes	yes	100	Magn. field transmission
X-ray topography	Synchr.	1000	–	yes	Volume	Magn. field transmission
SEMPA	Electrons	50	–	no	30	

Photoemission microscopes are instruments closely related to low-energy electron microscopes (LEEMs) which have been developed over the last few decades mostly at the Technical University of Causthal in Germany [12]. Any LEEM instrument may be used for photoemission microscopy by simply using UV or soft x-rays for excitation rather than monochromatic electrons. These instruments usually comprise also an energy analysis, which allows for higher spatial resolution and also provides the possibility to acquire images using primary photoelectrons of well defined energetic width. This may be used to achieve enhanced surface sensitivity in comparison to total yield microscopy.

4. Ferromagnetic domains at surfaces imaged by PEEM

Figure 5 shows a domain image of a 20 nm Fe film grown on Ge(100) [17]. One recognizes that the domains are elongated, with the long axes oriented along a specific direction. Without further information, one might interpret the image in terms of domains with magnetizations parallel to this elongated axis. One way to determine the magnetization directions unambigously is to study the dependence of the magnetic contrast on the azimuthal orientation of the sample. The contrast should be maximum when the magnetization lies in the incidence plane of the light, and it should vanish when the magnetization in a domain is perpendicular to the incidence plane. However, azimuthal rotation of the sample is not always possible, and in addition the acquistion of a series of images at different azimuthal settings is rather time consuming. An alternative route is to determine the magnitude of the magnetic contrast in different domains by taking spatially resolved absorption spectra. For this purpose, one defines regions in the image lying in different domains, and measures the electron yield just in these regions as a function of photon energy. By comparing absorption spectra taken with right and left circular light, the magnitude of the magnetic contrast can be determined. This is shown in the lower panel of figure 5. One finds that the bright domains show a large magnetic dichroism, whereas the absorption spectra for dark domains are virtually identical for right and left circular polarized light. Taking the angle of incidence and the finite degree of light polarization into account, the dichroism for the bright domains amounts to 28%. This is close to the value found for fully magnetized Fe, and shows that the magnetization in these domains lies within the plane of incidence. As the dark domains show no dichroism, the magnetization in these regions is at a right angle to the plane of incidence. Therefore, the domains are of the 90° type, and not 180°. The irregular shapes of the doains are related to the relatively large thickness of the film, where the energetic differences between different wall geometries are smaller than for ultrathin films.

Most experimental techniques give only information on the magnetic domain pattern at the surface of a sample. The thickness of the layer probed by different techniques varies, and depends first of all on the probe used. Conventional magneto-optical techniques have a probing depth of about 100 nm on metals. Nevertheless, the sensitivity of magneto-optics has been developed to a stage where monolayers may be detected when they are supported on a non-magnetic substrate. However, if one wants to study magnetic order in an ultrathin film absorbed on a ferromagnetic substrate, conventional magneto-optics is not applicable since the magnetic Kerr signal would be dominated by the ferromagnetic substrate. In this context the chemical specificity of XMCD microscopy is extremely useful since the magnetic signal detected at an absorption edge of the adsorbate provides information only on the adsorbate, without influence of the substrate on the measured signal. Figure 6 illustrates this capability for an Fe surface onto which a sub-monolayer of Mn was deposited [18]. The upper image shows the domains of a ferromagnetic Fe(100) film grown on Ag(100). The light was tuned to the Fe 2p absorption edge, and the non-magnetic contrast was removed by forming the asymmetry between images obtained with right and left circular light polarization. The brightest and darkest regions show domains whose magnetization is either parallel or antiparallel to the light polarization, which coincides with the direction of light propagation. The intermediate contrast level shows domains whose magnetization is at a right angle to the light incidence. The shape anisotropy of ultrathin films ensures that the magnetization lies within the film plane. This can be established from the magnitude of the magnetic dichroism which should only depend on the angle of light incidence onto the sample and the azimuthal sample orientation. For the film studied in figure 6 this is indeed the case; the magnetization lies within the film plane. Furthermore, one observes that the borders between domains, the domain walls, form nearly

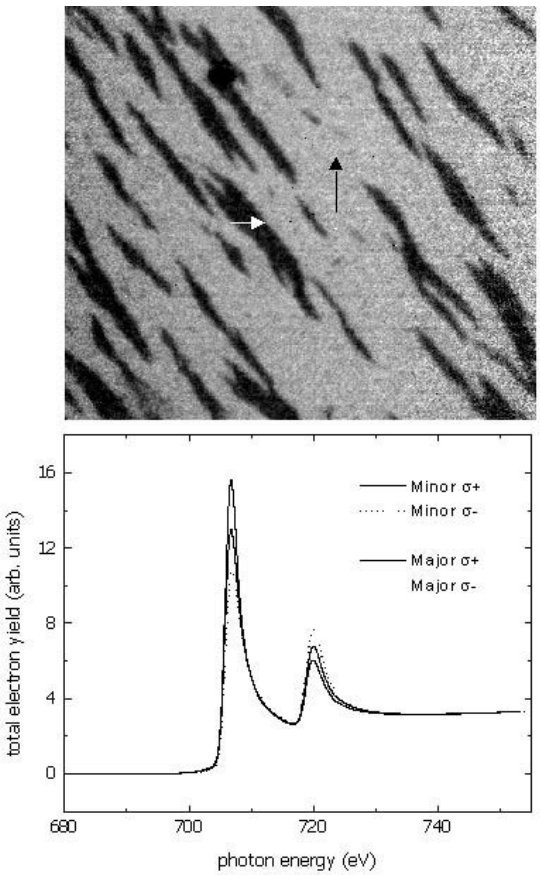

Figure 5. Magnetic domains in a 20 ML film of Fe on Ge(100). Images taken at the Fe 2p threshold, light is incident from below, the field of view is 35 μm wide. The lower panel shows XMCD absorption spectra for the Fe 2p edge. The spectrum of the domains appearing dark remains essentially unchanged on magnetization reversal, whereas that of the bright domains displays the full contrast of 28% [17].

straight lines, and occur primarily in two directions forming an angle of 90° to each other. This finding reflects the crystalline anisotropy of Fe which governs the in-plane domains of this epitaxial Fe film. In bulk Fe, the directions of easy magnetization are the (100) directions, so for the thin film we expect the magnetization to lie parallel to in-plane 10 and 01 directions. This is in agreement with the overall picture observed in figure 6. Furthermore, we find that the domain walls run parallel to the in-plane 11 directions. This means that magnetization direction changes by 90° across a domain wall: therefore the walls are called 90° walls. It is apparent that there are only 90° walls. This reflects the fact that for an Fe thin film 180° would have higher energy. The internal structure of the domain walls is of high interest as it allows quantitative conclusions about the magnetic anisotropy and its deviations from the bulk in the vicinity of the surface.

The properties of ultrahtin films in the monolayer range may deviate strongly from those of the bulk material. The basic cause for such modifications of the properties is the reduced coordination of the atoms in the surface layer. This leads to a narrowing of the electronic energy

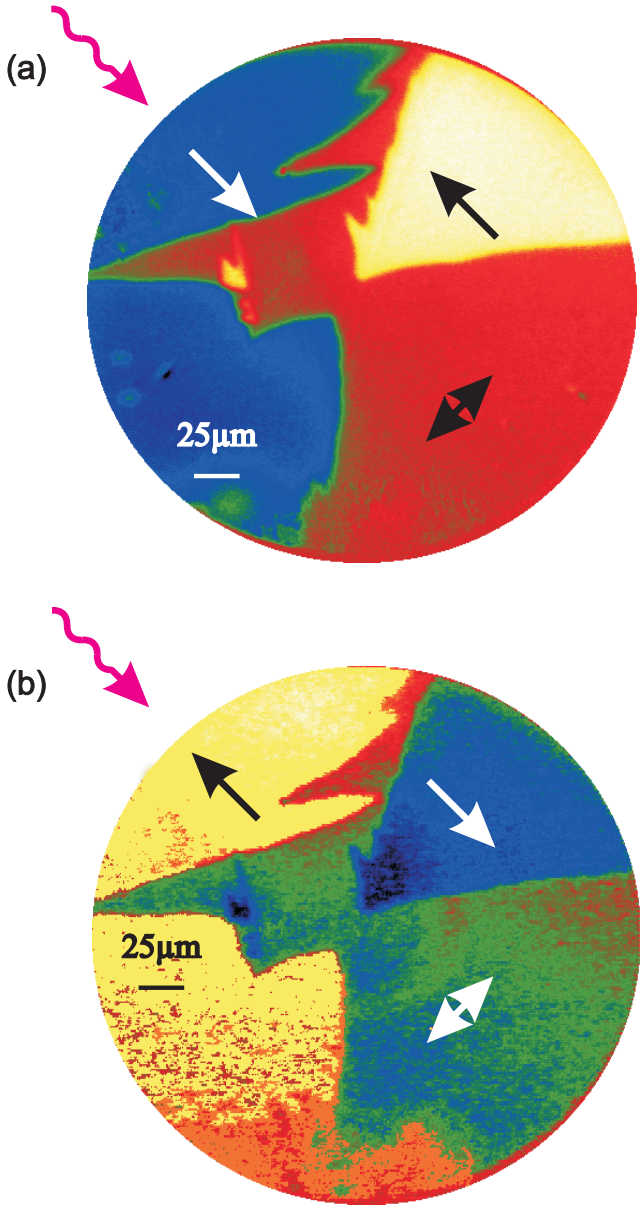

Figure 6. Magnetic domains for a bilayer 0.25 ML Mn/15 ML Fe/Ag(100). Upper panel shows domains of Fe substrate, lower shows image obtained at the Mn 2p edge (from [18]).

bands, which may be sufficient to support magnetism. Such phenomena were first predicted from calculations of the electronic properties of monolayers supported on various substrates. Also the magnetic properties of sufaces may deviate strongly from the bulk, primarily with respect to the magnitude of the magnetic moment. Experimentally, phenomena of this type are difficult to detect since the ordering temperature of an ultrathin film in the monolayer regime would probably be extremely low. The situation is different if the ultrathin film is supported on a magnetic substrate. Of course, this changes the physics in a profound way

since in addition to hybridization between the electronic states of the film and substrate one introduces an exchange interaction between film and substrate atoms. Therefore it may be anticipated that the magnetic order in such a thin film is largely governed by the magnetic properties of the substrate. Nevertheless, such systems constitute an interesting subject for experimental studies just because of this exchange coupling. Cr and Mn as bulk materials are antiferromagnetic, so thin films of these metals may be expected to show magnetic order. To study the exchange interaction between monolayer films of these metals on magnetic substrates, the chemical specificity is essential. The lower panel of figure 6 shows a photoemission image obtained after depositing a quarter of a monolayer of Mn on the Fe surface. To investigate the exchange coupling between substrate and adsorbate, the photon energy was tuned to the Mn 2p absorption edge. An asymmetry image was formed from images taken with both light helicities. The magnetic contrast revealed by the asymmetry image shows the same domain pattern as observed before for the Fe substrate, albeit with inverted contrast. This demonstrates antiferromagnetic coupling between the magnetic moments of the Mn adsorbate and those of the Fe substrate. The antiferromagnetic coupling was also confirmed by taking complete dichroism spectra on the magnetically saturated sample, and by the observation of inverted hysteresis loops at the Fe and Mn edges [18]. Previously, the spin polarization in the Mn 3p core level photoemission spectrum had been measured which also indicated antiparallel coupling between Fe and Mn [19]. A number of calculations have been carried out addressing the properties of Fe/Mn interfaces [20–22]. There appears to be a consensus that the complete Mn monolayer on Fe(100) has an antiferromagnetic ground state. This is in agreement with the experiment, as no magnetic Mn signal was observed for coverages of a full monolayer or more. If there is no segragation, submonolayer coverages may be modelled by isolated atoms adsorbed on the Fe(100). For such a system, theory finds both a ferro- and an antiferromagnetic state as ground state, depending on whether the Mn atom is placed in the surface layer of the crystal, or situated in a genuine adsorption site above the surface layer [21]. The energy difference between these two states is very small. The sign of the coupling observed in a specific experiment—ferro- or antiferromagnetic—probably depends on the morphology of the adsorbed layer, which probably depends on the substrate roughness, the degree of intermixing, etc. Similar studies have been carried out for Fe/Cr/Fe sandwich structures with variable Cr thickness to characterize the interlayer exchange coupling [23]. Recently, the spin reorientation transition of ultrathin Ni(100) films from perpendicular to in-plane magnetization was studied by PEEM [24]. Since the magnetic anisotropy is related to the orbital magnetic moment, the possibility to extract quantitative information on the magnetic moment in a spatially resolved way provided the key to a comprehensive characterization of this phenomenon.

5. Antiferromagnetic domains

As pointed out in the introduction, antiferromagnetic materials in general also exhibit magnetic domains. An antiferromagnet can be considered as being composed of a number of sublattices consisting of ferromagnetically ordered sites, whose magnetizations cancel. In the simplest case, there are just two sublattices with opposite magnetization. In this case the antiferromagnetic structure is collinear. As the Néel temperature is approached, the sublattice magnetizations decrease and finally vanish. Since the magnetization is zero for an antiferromagnet, one has to use a different physical quantity as order parameter. As an order parameter, the difference of the sublattice magnetizations, called the AF vector, is a suitable choice. Antiferromagnetic domains are characterized by different orientations of the AF vector.

Because of the vanishing magnetization, antiferromagnetism and the domains associated with it are more difficult to detect than ferromagnetic ones. The classical method to detect antiferromagnetism is neutron scattering [25]. This technique has also been applied to image AF domains in topographic experiments [26]. However, because of the long data acquisition periods needed to obtain a topogram—a few tens of hours—and the obtainable resolution—40 μm—other methods are highly desirable. The AF ordered state is in many cases accompanied by a distortion of the crystal due to magnetostriction (or exchange striction). This can monitored by x-ray diffraction or also linear birefringence in the optical regime. However, none of these techniques is surface sensitive, chemically specific, fast, and suitable for high-resolution imaging. All the synchrotron based methods listed in table 1 are also able to detect antiferromagnetism. This is based on the possibility to exploit linear magnetic dichroism in x-ray absorption [27–29]. This dichroism occurs as a change of the absorption spectrum on the for linear light polarization being either parallel or perpendicular to the magnetic moment.

In the following we will discuss the imaging of antiferromagnetic domains of NiO by photoemission microscopy, utilizing linear magnetic dichroism in x-ray absorption. NiO crystallizes in the rock salt structure, which undergoes a small distortion below the Néel temperature. The antiferromagnetic structure of NiO consists of ferromagnetic 111 sheets, which are stacked in an antiferromagnetic sequence, thereby forming a collinear antiferromagnet [25]. Since there are four different 111 directions, there are four different antiferromagnetic domains. The magnetic moments carried by the Ni 2+ ions lie within the ferromagnetic 111 sheets along the $\underline{2}11$, $1\underline{2}1$, $11\underline{2}$, etc. type directions. AF domains are firstly associated with different 111 directions as stacking directions. Since the distance between the antiferromagentically stacked 111 sheets is contracted due to magnetostriction, domains of this type form crystallographic twins. Therefore these domains are called T domains. Furthermore, domains may arise from different spin orientations wihin a particular T domain, which are called S domains. As there are four T domains, each comprising three different S domains, there are in total twelve different domains possible in NiO [30].

To observe linear magnetic dichroism in an antiferromagnetic system without spatial resolution, one has to find a way to prepare the sample to exhibit a macroscopic region with a preferred antiferromagnetic axis. Alders *et al* achieved this by studying thin films of NiO grown epitaxially on MgO [28, 29]. The thin film nature of the sample, in combination with the small lattice mismatch between NiO and MgO was expected to generate an anisotropy which might lead to a preferred orientation of the magnetic moments. If such a mechanism is effective, it should be detectable by a polarization dependence of the absorption spectrum. Experimental studies on NiO films did indeed reveal different Ni 2p absorption spectra with normal or grazing incidence of linearly polarized light. The absorption spectra were taken by monitoring the total electron yield as a function of photon energy. The observed polarization dependence was in agreement with calculations, assuming that of the twelve possible AF domains in NiO, only those with a large magnetic moment normal to the film plane are present. The polarization dependence was observed to disappear above the Néel temperature, which in turn was found to be lowered for thin films. Figure 6 shows the Ni 2p absorption spectrum of NiO. Two prominent structures arise from $2p_{1/2}$ and $2p_{3/2}$ final state holes. Both absorption structures show fine structure which is caused by Coulomb and exchange interaction between the 2p core hole and the magnetic valence electrons [31]. The line shape is in agreement with calculations incorporating these interactions. From such calculations it is found that the detailed line shape depends on the relative orientation of light polarization and magnetic moment of the Ni atom which absorbs the photon. Both edges in principle show such a dependence. The Ni $2p_{1/2}$ edge consists of two peaks whose intensity ratio changes with a change of the angle between polarization and Ni magnetic moment. Alders *et al* [28, 29] found in their study on thin

films that the intensity ratio between these two structures changes in a systematic way with the angle of light incidence. This showed that the films consisted primarily of domains with large projection of magnetic moment normal to the film plane. However, no dependence of the absorption spectrum on the lateral position on the sample was found. This demonstrated that the domains were smaller that the 1 mm light spot.

Spatially resolved studies of the Ni 2p absorption edge with the goal of imaging AF domains were carried out on ultrathin films grown on Ag(100) [32] and MgO(100) substrates [33]. In both cases the intrinsic domains were too small to be visible in microscope images. The intrinsic domain size in bulk NiO crystals is, however, suitable for imaging by photoemission microscopy. Figure 7 shows a collection of images of a NiO(100) surface covering an area of about 200×300 μm. Each image is constructed by division of two images taken with the light tuned to the two features of the Ni $2p_{1/2}$ absorption edge. Therefore the greyscale represents the intensity ratio of these two features of the absorption spectrum. The two grey levels show the presence of antiferromagnetic domains. These domains are found in the form of stripes running along [10] and [01] directions at the (100) surface of the crystal. The light was s polarized, i.e. with the electric field vector lying in the plane of the sample surface, parallel to the horizontal edges of the image. Therefore, one can conclude that one set of domains has large projection of the magnetic moment in the horizontal direction, whereas the magnetic moments in the other direction is close to the vertical axis. Rotation of the sample about its surface normal changes the angle between light polarization magnetic moments, thereby also affecting the magnetic contrast. From a comprehensive study of this polarization dependence one can conclude that on a cleaved surface and for the domains seen in figure 8, the magnetic order at the surface is bulk terminated [34].

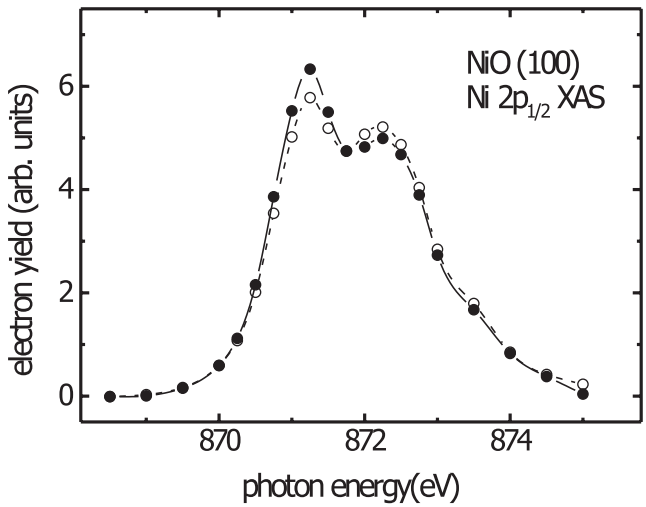

Figure 7. Ni $2p_{1/2}$ absorption spectrum of NiO measured by total yield with s- and p-polarized light. The measurement was carried out on a surface cleaved freshly in UHV (from [17]); open and filled symbols are for different domains of the microsocpe image.

A study of the temperature dependence of the observed contrast shows that within experimental accuracy it disappears at the bulk Néel temperature. However, the temperature dependence differs markedly from the bulk temperature dependence of AF order as measured by neutron scattering [34]. A similar surface behaviour as reported here from the PEEM data has been found in a LEED study where the intensity of the superstructure reflections induced

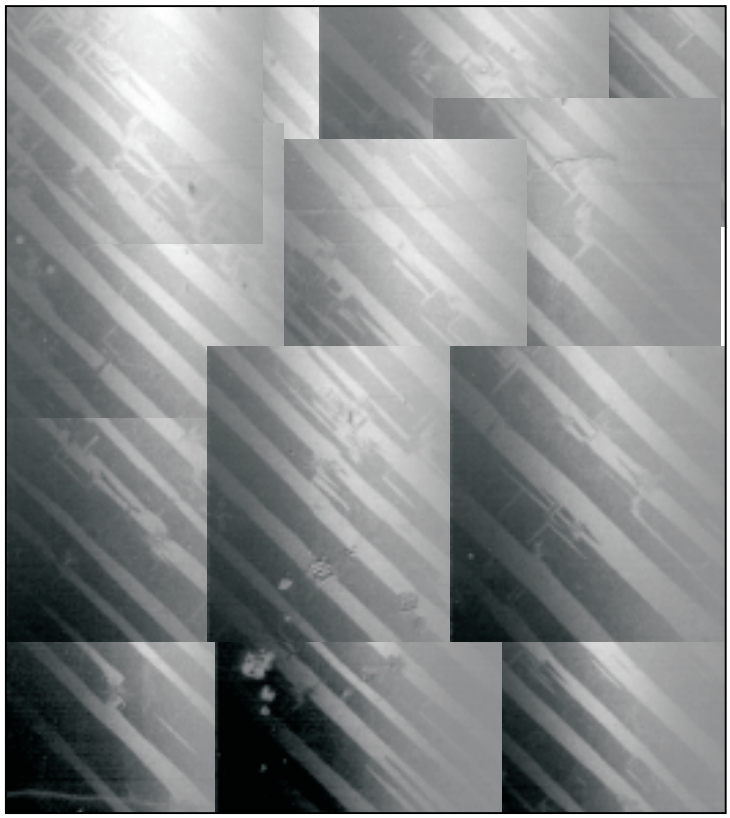

Figure 8. Antiferromagnetic domains at the (100) surface of NiO, imaged by linear magnetic dichroism at the Ni $2p_{1/2}$ absorption edge. The field of view is about 250 μm across. The resolution in this image is about 100 nm.

by the doubling of the unit cell in the antiferromagnetic state was used as a measure for the AF order parameter [35]. The deviation of the surface temperature dependence from that of the bulk can be explained within a molecular field model with a reduced exchange interaction at the surface.

Imaging of antiferromagnetic domains by linear magnetic dichroism in photoemission microscopy opens the field of antiferromagnetism at surfaces and interfaces to detailed investigations which were not possible with the previously available methods [36–38]. An example which is relevant to technological issues is the interface between an antiferromagnet and a ferromagnet. Figure 9 shows the ferro- and antiferromagnetic domains for a thin layer of Co deposited on NiO(100). The antiferromagnetic domains show the same stripe pattern as discussed above. To image the ferromagnetic domains in the Co film, the circularly polarized light is tuned to the Co 2p edge. The image shows stripes of identical shape as the AF domains. In the regions corresponding to the bright AF domains, one observes strong ferromagnetic domains contrast. This indicates that the magnetitization in these domains is parallel or antiparallel to the light, which is incident parallel to the vertical axis of the image.

Within the regions corresponding to the dark AF domains, there is no ferromagnetic contrast observable in the internal. However, the signal level is intermediate between the levels of the other ferromagnetic domains. This indicates that the magnetization is perpendicular to the direction of light incidence. Combining this with the information on the antiferromagnetic domains leads to the conclusion, that the coupling between the moments of NiO and the Co film is collinear. Detailed analysis shows that the near surface magnetic structure of the NiO is modified by the presence of ferromagnetic Co [37]. Studies on other ferro–antiferromagnetic interfaces have been reported.

6. Summary and outlook

Imaging of magnetic domains, micro- and nanostructures by microscopic techniques utilizing synchrotron radiation is still undergoing a rapid development. The examples discussed in this necessarily incomplete review illustrate the capabilities of these techniques. X-ray microscopy allows us to apply a magnetic field to the sample, which is important for many problems. On the other hand, the samples have to be prepared as very thin layers on a suitable carrier. This is not necessary for photoemission microscopy, but the sample only has to be conducting, which is not needed in x-ray microscopy. The limited escape depth of the secondary electrons makes this method of imaging much more surface sensitive. The tunability and polarization of the synchrotron radiation is in both cases a necessary prerequisite. For numerous problems the methods discussed here offer a unique access to the problem. Examples are the investigation of inhomegenous samples, e.g. layered structures, where the chemical specificity can be used to differentiate between different components. The possibility to perform time resolved studies will probably be explored in the future. In this context, pump-probe experiments for the characterization of dynamic properties are of particular interest. Photoemission microscopy offers a very simple way to image antiferromagnetic domains at surfaces, which opens the possibility to study antiferromagnetism at surfaces in a simple way.

The ongoing development of microscopes with ever better resolution will open the field for more sophisticated studies. In the near future new photoemission microscopes will become operational with unprecedented resolution. The SMART (standing for 'spectromicroscope for all relevant techniques') project at BESSY II is designed for an ultimate resolution of 2 nm [39, 40]. The instrument is being built at a specifically designed undulator beamline covering the energy range from 20 to 2000 eV with a maximum energy resolution of $\Delta E/E = 10^4$. Even though the undulator and beamline are designed to deliver linear polarized light to the sample, magnetic imaging will be possible by making use of linear magnetic dichroism. In the total yield mode this may be done—as discussed above for NiO—on materials with highly localized d states. In metallic systems, linear dichroism is very small in absorption, and it is more attractive to make use of linear magnetic dichroism in core level photoemission spectra [41], whose magnitude is an uneven function of the magnetization. A similar instrument, the PEEM 3, which is under construction at the Advanced Light Source in Berkeley, is also aiming for a resolution of two nanometres. As with the SMART, the PEEM 3 instrument will also include a magnetic beam separator and electrostatic mirror. The undulator will offer linear as well as circularly polarized light, which makes the instrument very versatile for studies of magnetic materials.

For imaging of magnetic domains also other high resolution techniques are available, e.g. magnetic force microscopy (MFM) [42], magneto-optical scanning near field microscopy (SNOM) [43], or spin-polarized scanning tunnelling microscopy (sp-STM) [44, 45]. While the two former techniques achieve typically a resolution of a few tens of nm, scanning tunnelling microscopy is capable of achieving atomic resolution. Photoemission microscopy offers

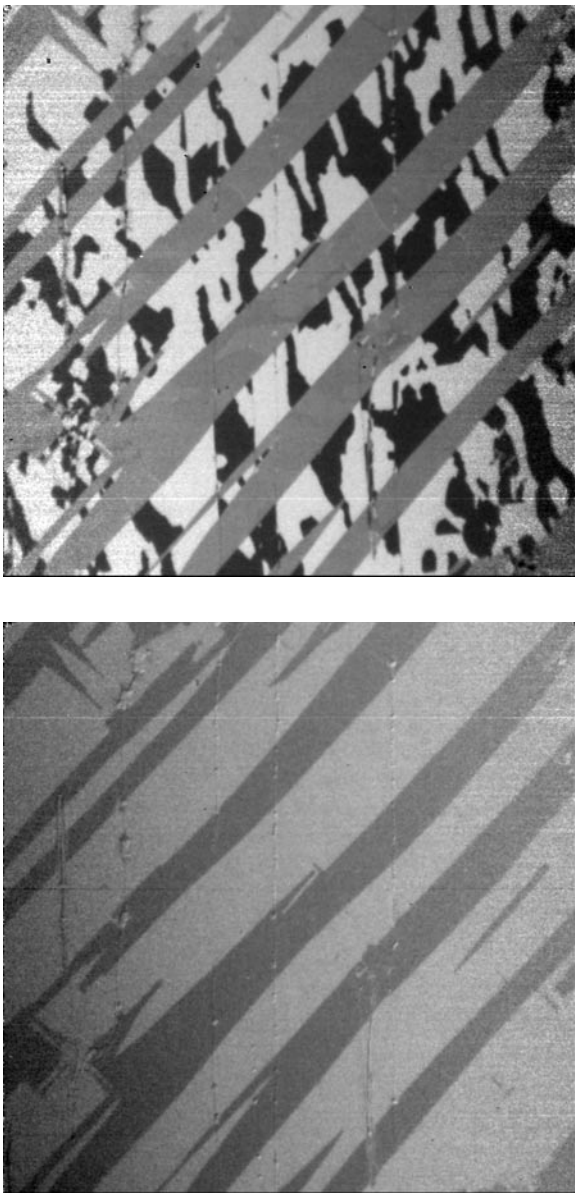

Figure 9. Magnetic domains for Co/NiO(100). The bottom panel shows the antiferromagnetic domains of NiO imaged by linear magnetic dichroism. The top panel shows ferromagnetic domains in the Co film imaged by circular dichroism at the Co 2p edge. The analysis shows that there is a collinear coupling between the moments of the antiferromagnet and the ferromagnet (from [37]). The resolution in this image is about 100 nm.

comparable resolution to that of MFM or magneto-optical SNOM, but cannot compete with atomic resolution offered by sp-STM. However, PEEM offers some features which are unique to this technique. This is the chemical specficity, and the ability to image buried layers. This may be used either to analyse materials which come out of a technical production process, and are covered by a contaminating layer, or to characterize multilayered samples where the

interaction between domains on different layers is of interest. Furthermore, the pulsed nature of synchrotron radiation allows for dynamical investigations in a stroboscopic mode with an ultimate time resolution given by the length of the light pulse generated by the synchrotron, which is of the order of 50 ps for a third-generation source. Possible areas where these advanced instruments will be employed are the study of individual non-sized planar magnetic elements, where the small size strongly influences both the static and dynamic magnetic properties.

Acknowledgments

The author is indebted to all collaborators in his group who participated in his experiments in this field, in particular to H Ohldag and N B Weber, without whose enthusiasm the experiments on antiferromagnetic materials would not have been possible. Furthermore it is a pleasure to acknowledge the support of colleagues BESSY, Hasylab, the ESRF, and the ALS, as well as fruitful and informative discussions with colleagues working in this field.

References

[1] Hubert A and Schäfer R 1998 *Magnetic Domains* (Berlin: Springer)
[2] Chen C T, Sette F, MA Y and Modesti S 1990 *Phys. Rev.* B **42** 7262
[3] Chen C T, Idzerda Y U, Lin H J, Smith N V, Meigs G, Chaban E, Ho G H, Pellegrin E and Sette F 1995 *Phys. Rev. Lett.* **72** 152
[4] Gudat W and Kunz C 1972 *Phys. Rev. Lett.* **29** 169
[5] Eimüller Th, Kalchgruber R, Fischer P, Schütz G, Guttmann P, Schmahl G, Köhler M, Prügl K, Scholz M, Bammes F and Bayreuther G 2000 *J. Appl. Phys. 87* 6478
[6] Voss J, Kunz C, Moewes A and Storjohann I 1992 *Rev. Sci. Instrum.* **63** 569
[7] Friedrich J, Rozhko I, Voss J, Hillebrecht F U, Kisker E and Wedemeier V 1999 *J. Appl. Phys. 85* 4610
[8] Pretorius M, Friedrich J, Ranck A, Schroeder M, Voss J, Wedemeier V, Spanke D, Knabben D, Rozhko I, Ohldag H, Hillebrecht F U and Kisker E 1997 *Phys. Rev.* B *55* 14133
[9] Hillebrecht F U, Kinoshita T, Spanke D, Dresselhaus J, Roth Ch, Rose H B and Kisker E 1995 *Phys. Rev. Lett.* **75** 2224
[10] Engel W, Kordesch M E, Rothermund H H, Kubala S and von Oertzen A 1993 *Ultramicroscopy* **36** 16
[11] PEEM 350 by Staib Instruments, Langenbach, Germany
[12] Marx G K L, Elmers H J and Schönhense G 2000 *Phys. Rev. Lett.* **84** 5888
[13] Anders S, Padmore H A, Duarte R M, Renner T, Stammler T, Scholl A, Scheinfein M R, Stöhr J, Séve L and Sinkovic B 1999 *Rev. Sci. Instrum.* **70** 3973
[14] Bauer E 2001 *J. Phys.: Condens. Matter* **13** XXXX
[15] Solinus V 1997 *Diploma thesis* Düsseldorf, unpublished
[16] Berger A and Oepen H P 1992 *Phys. Rev.* B **45** 12596
[17] Ohldag H and Hillebrecht F U 2001 to be published
[18] Dresselhaus J, Spanke D, Hillebrecht F U, Kisker E, van der Laan G, Brookes N B and Goedkoop J B 1997 *Phys. Rev.* B **56** 5461
[19] Roth Ch, Kleemann Th, Hillebrecht F U and Kisker E 1995 *Phys. Rev.* B **52** R15691
[20] Wu R and Freeman A J 1995 *Phys. Rev.* B **51** 17131
[21] Nonas B, Wildberger K, Zeller R and Dederichs P H 1997 *J. Magn. Magn. Mater.* **165** 137
[22] Elmouhssine O, Moraitis G, Demangeat C and Parlebas J C 1997 *Phys. Rev.* B **55** R7410
[23] Frömter R 2001 *PhD thesis* Halle, unpublished
[24] Kuch W, Gilles J, Kang S S, Imada S Suga S and Kirschner J 2000 *Phys. Rev.* B **62** 3824
[25] Roth W L 1958 *Phys. Rev.* **111** 772
[26] Baruchel J, Schlenker M, Kurosawa K and Saito S 1981 *Phil. Mag.* B **43** 853
[27] Kuiper P, Searle B G, Rudolf P, Tjeng L H and Chen C T 1993 *Phys. Rev. Lett.* **70** 1549
[28] Alders D, Vogel J, Levelut C, Peacor S D, Hibma T, Sacchi M, Tjeng L H, van der Laan G, Thole B T and Sawatzky G A 1995 *Europhys. Lett.* **32** 259
[29] Alders D, Voogt F C, Hibma T and Sawatzky G A 1996 *Phys. Rev.* B **54** 7716
[30] Yamada T 1966 *J. Phys. Soc. Japan* **21** 650
[31] van der Laan G *et al* 1986 *Phys. Rev.* B **33** 4523

[32] Spanke D, Knabben D, Solinus V, Hillebrecht F U, Ciccacci F, Gregoratti L and Marsi M *Phys. Rev.* B **58** 5201
[33] J. Stöhr, Scholl A, Regan T J, Anders S, Lüning J, Scheinfein M R, Padore H A and White R L 1999 *Phys. Rev. Lett.* 1862
[34] Hillebrecht F U, Ohldag H, Weber N, Bethke C, Mick U, Weiss M and Bahrdt J 2001 *Phys. Rev. Lett.* **86** 3419
[35] Wolfram T, DeWames R, Hall W and Palmberg P 1971 *Surf. Sci.* **28** 45
[36] Scholl A, Stöhr J *et al* 2000 *Science* **287** 1014
[37] Ohldag H, Scholl A, Nolting F, Stöhr J and Hillebrecht F U 2001 *Phys. Rev. Lett.* **86** 2878
[38] Nolting F, Scholl A, Stöhr J *et al* 2000 *Nature* **405** 767
[39] Fink R, Weiss M R, Umbach E, Preikszas D, Rose H, Spehr R, Hartel P, Engel W, Degenhardt R, Wichtendahl R, Kuhlenbeck H, Erlebach W, Ihmann K, Schlogl R, Freund H-J, Bradshaw A M, Lilienkamp G, Schmidt T, Bauer E, Benner G 1997 *J. Electron Spectrosc. Relat. Phenom.* **84** 231–50
[40] Wichtendahl R, Fink R, Kuhlenbeck H, Preikszas D, Rose H, Spehr R, Hartel P, Engel W, Schlögl R, Freund H-J, Bradshaw A M, Lilienkamp G, Bauer E, Schmidt T, Benner G and Umbach E 1998 *Surf. Rev. Lett.* **5** 1249–56
[41] Roth Ch, Hillebrecht F U, Rose H B and Kisker E 1993 *Phys. Rev. Lett.* **70** 3479
Hillebrecht F U, Roth Ch, Rose H B, Park W G, Kisker E and Cherepkov N A 1996 *Phys. Rev.* B **53** 12182
[42] Hartmann U, Göddenhenrich T and Heiden C 1991 *J. Magn. Magn. Mater.* **101** 263
[43] Betzig E, Trautman J K, Wolfe R, Gyorgy E M, Finn P L, Kryder M H and Chang C-H 1991 *Appl. Phys. Lett.* **61** 142
[44] Bode M, Getzlaff M and Wiesendanger R 1998 *Phys. Rev. Lett.* **81** 4256
[45] Wulfhekel W and Kirschner J 1999 *Appl. Phys. Lett.* **75** 1944